https://erjm.journals.ekb.eg
ISSN: 1110-1180

DOI: ---------

ERJ
Engineering Research Journal
Faculty of Engineering
Menoufia University

A Fuzzy Logic Based Maximum Power Point Tracking of PV Systems Supplying Remote Sensing Devices of Two Units Cube Satellite Applications

Mohamed E. Attalla[1], Ragab A. El-Sehiemy[2], Hasnaa M. El Arwash[3*]

[1] Electronics and Communication Engineering Department, Alexandria higher Institute of Engineering & Technology Egypt
[2] Electrical Engineering Department, Faculty of Engineering-Kafr Elsheikh University, Egypt
[3] Mechatronics Engineering Department, Alexandria higher Institute of Engineering & Technology, Egypt
(Corresponding author: hasnaa.mohamed@aiet.edu.eg)

ABSTRACT
The primary goals of remote sensing of satellites are extending their lifetime, improving their resolution, decreasing the cost and corresponding weight. Using the maximum power point tracking (MPPT) technique can help to achieve the primary goals, including decreasing the weight and the reduction of satellites cost. In this regard, this paper aims to optimize the MPPT technique while taking into account the uncertain change of environmental conditions, such as solar irradiation, ambient temperature, air mass angle, and the arrangement method of the cells to construct the solar array system's panels. The fuzzy logic controller (FLC) is investigated to modulate the pulse width modulation's duty cycle to control a boost DC-DC converter. As a result, the proposed FLC based MPPT technique achieves the primary goals. The modeling and simulation environment used to implement the suggested model, based multicrystal KC200GT PV modules, was MATLAB/Simulink R2022. Numerical findings highlight approximately 99.8% accuracy with a 0.02 s best response time of the mathematical modeling at different environmental conditions.

Keywords: *environmental operating conditions, fuzzy logic controller, maximum power point tracking, PV modules, satellite power supply.*

1. Introduction

Energy systems such as solar cells are the most desirable type of regenerated energy available. Moreover, it could be considered one of the most valuable sources due to numerous advantages such as pollution-free operation and reduced costs of maintenance, which promise to increase their share in the near future. According to an International Energy Agency (IEA) report that examined global demand of energy, about 40 - 60 Terawatts of solar energy per year by 2050 are predictable [1]

Energy demand per day is increasing, and to satisfy those requirements, energy is typically produced using non-renewable conventional resources such as coal, diesel, natural gas, and so on [2]. As a result, there are large emissions of carbon dioxide that were produced with the usage of conventional resources. The use of renewable energy sources is rising as more nations choose to collaborate with zero-carbon countries [3]. Solar panel usage is rapidly increasing due to the free abundance of solar energy, especially in satellites with an accurate design of their controllers that grantee the sustainability of the satellite power supply as possible [4]. The solar panel, on the other hand, has an efficiency of 13-19%. the effectiveness of the maximum power point tracking (MPPT) technique (above 98%) and the inverter efficiency (roughly 95–98%) [5]. Sudden shifts in the atmospheric conditions and the circuits they are connected to, including loads, charge controllers, and other devices, are too uncertain blame for these low efficiencies [6]. In photovoltaic (PV) systems, MPPT is used to maximize the power produced by the SA and minimize the probability of a mismatch between the operating characteristics of the load and the SA [7-11].

Although many algorithms are created, conventional techniques like P&O and incremental conductance (INC) are still frequently employed due to their ease of use; nevertheless, these techniques lead to more energy losses [12]. The advancement of microcontrollers and computational methods have led to the creation of several techniques like ant bee colonies, neural networks, fuzzy logic, particle swarms, hybrid models, ANFIS, and more. The references provide information on several conventional MPPT techniques, including fractional open circuit voltage (FOCV) [13], and fractional short circuit current (FSCC)

[14], curve fitting [14], hill climbing (HC) [15] and the INC [16]. The most significant shortcomings of FOCV and FSCC are primarily utilized for low-power applications, which makes them less precise [13, 14]. Common methods like P&O, INC, and HC behave well. Still, they are useless in situations with fluctuating irradiation and shading because they can only generate their maximum power in conditions of constant insolation [15, 16]. These methods also have poor convergence, a higher number of steady-state oscillations, and slow MPP tracking [17].

Transient behavior of Intelligent MPPT techniques like neural networks, fuzzy logic, and ANFIS are used to enhance effectiveness in the steady state [18, 19]. Fuzzy controllers, which offer high performance control at a high computational burden and a limited application in complex systems, have been proposed to solve the problems associated with PI controller [20]. In [21], the ANFIS technique combines the merits of fuzzy logic and neural networks, but to obtain such good accuracy, more numerical calculations in the training phase, this is extremely hard; if the trained process error is not a part of 10000, the response of the hybrid models will be inaccurate as it will contain high oscillations [22]. In the P&O method with multi-layer Artificial Neural Network (ANN) , there is a big challenge in the model training and the collection of the datasets [23].

Table 1–Assessment of previous MPPT controllers

Controller type	Ref.	Merits	Limitations
P&O	[8]	• Straightforward design • Ease of operation and execution	• I was unable to follow the MPP in the face of steep variations in the atmosphere.
Incremental Conductance Method	[2, 3]	• It can calculate the maximum power point without fluctuating around it.	• It can exhibit erratic behavior and oscillate in situations where the atmospheric conditions change quickly. • Extended computation times
Fuzzy Inference System (FIS)	[22]	• The training procedure involves more difficult numerical computations for precise results;	• An increased number of oscillations can be found in the hybrid models' erroneous response if the algorithms are not sufficiently trained.
Grey Wolf Optimization (GWO)	[29, 30]	• Limited parameters. • Easy to understand principles. • Easy implementation.	• Convergence occurs slowly. • The solution's accuracy is low. • It is extremely easy to fall into the local optimum.
GA	[24, 25]	• Finding the best viable solutions. • Dealing with complex problems.	• Expensive computationally. • May not always guarantee the global optimum
PSO	[26-28]	• There are fewer parameters to adjust. • Determines the best solution based on particle interaction.	• It converges slowly to the global optimum through a high-dimensional search space. • Furthermore, it produces low-quality results for complex and large datasets.
Neural Network Method	[42, 43]	• With variable loads, steady radiation treatments, and a constant temperature, it took almost 0.05 seconds.	• There may be disruptions at the output's constant points.
ANFIS	[22-25]	• Dimensionality course. • Training parameters and ensuring rules are understandable.	• Easily applicable to larger problems.

Neural Network tracks MPP more quickly by altering layer weights in accordance with the learning algorithm. In terms of efficiency and reactions, NN controllers perform well in situations with rapidly changing illumination and partial shading [24]. Intelligent methods outperform conventional methods in terms of performance, and artificial intelligence mitigates the drawbacks of methods like genetic algorithms (GA) [24, 25], particle swarm optimization (PSO) [26-28], grey wolf optimization (GWO) [29, 30], and so on. But the intricacy of the implementation and design matters. Neural networks are a quick fix for increasing productivity because they can oversee problems with uncertainty and require no prior knowledge [23, 31].

The combination of two or more of the aforementioned methods results in a category known as hybrid methods, which boosts the models' efficacy. Numerous hybrid

models have been proposed, but their levels of complexity are varied depending on for the application that they used in. Examples include P&O with multi-layer ANN [32], ANN with a variable step size of P&O [33], GA, P&O with INC [34], Gravitational search algorithm with PSO, as well as numerous others.

To optimize the MPPT under different operating conditions, alternative techniques can be integrated with conventional techniques for reliable results [35-37]. By integrating these methods, output response uncertainties are reduced because P&O is simple to implement, and neural networks have accuracy and quick recovery times.

In this paper, a hybrid control that eliminates uncertainties found in P&O, INC, and other algorithms is proposed. Solar panel performance is enhanced with the use of the hybrid controller [38], and the combination that is part of the model gets rid of unreliable responses and offers a consistent performance in a variety of atmospheric conditions [39, 40]. The merits and demerits of previous methods that were reported in the literature was concluded in Table 1. As demonstrated from Table 1, it can be summarized that, The FLC, as stated in [41], is the most appropriate controller due to its small size, light weight, high accuracy, fast response, enough memory, and low computational load; all of which are crucial goals for satellites to meet.

In this paper, the fuzzy logic controller is developed to employ the MPPT tracker. The main contribution of this paper can be expressed as follows: for satellite, there are three modes of operation related to sunlight as shown in Fig. (1) [4]. In the following, a brief discussion about the three modes according to sunlight as demonstrated in Ref. [4]. In the first mode, the satellite controls the DC bus voltage based on the solar panels' MPPT operating condition. Also, the batteries are charged in accordance with their temperature and charging characteristics. In the second mode, the batteries can only charge and standby to discharge. The third mode occurs when the satellite's batteries run out of power during an eclipse [4].

Figure (2.a) depicts a two-unit cube satellite. CubeSats are a type of nanosatellite with standard size and form factor. The standard CubeSat size is a "one unit" or "1U" measuring 10x10x10 cms, which can be expanded to larger sizes of 1.5, 2, 3, 6, and even 12U. California Polytechnic State University at San Luis Obispo and Stanford University created the platform in 1999 to promote education and space exploration. CubeSat development has advanced to the point where government, industry, and academia are collaborating to increase capabilities. CubeSats now offer a low-cost platform for scientific research and technological demonstrations [44, 45]. Furthermore, Figure (2.b) shows where the various module components were placed. Every module is formed with basic components that let it meet the basic requirements for interconnected modules, as shown in Fig. (3). These components Are:

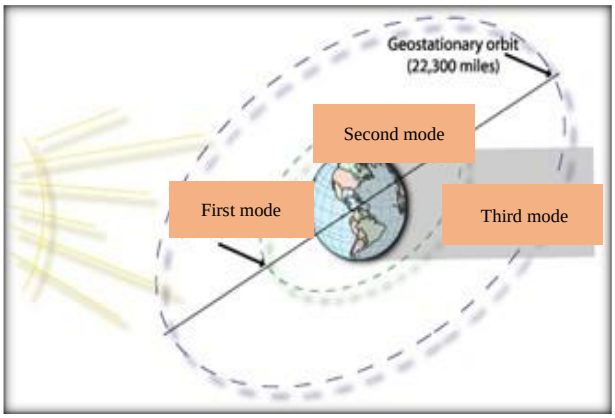

Fig. 1–The three modes of operation related to sunlight in LEO and GEO

• An ARM-based on-board computer (OBC) with commercial-of-the-shelf (COTS) components.
• A COTS switch to manage incoming traffic and data bus loops caused by interlinked interfaces. The switch is also responsible for informing the network about the topology of the module compound [44, 45].
• A Power Control Unit (PCU) with a battery is optional for powering components.
• Communicates with the Interface Control Unit (ICU) to dock with neighboring modules.
• Optional payload linked to Ethernet and power buses.

Since previous studies have confirmed that the exposure time of the satellite to the sun is noticeably short, and it is exposed to many variables such as solar radiation and temperature, it is necessary to provide an MPPT controller whose has fast response and high quality performance in the different environmental circumstances, lightweight, and small size as possible. The place in which the controller will be placed is as it is shown in Figure 2, which is exceedingly small. Fortunately, these features are available in Fuzzy logic MPPT as shown in the literature review in section 1.

The paper objective is to design and implement an optimal MPPT controller algorithm by considering the trade-offs made in earlier research as well as the constantly shifting environmental factors like air mass angle , atmospheric temperature , solar irradiation , and cell connection methods in the PV system's panels used for cube satellite

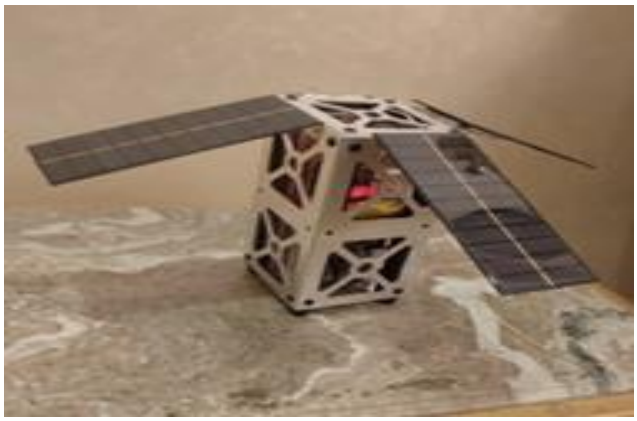

a. The two units cube satellite with solar panels

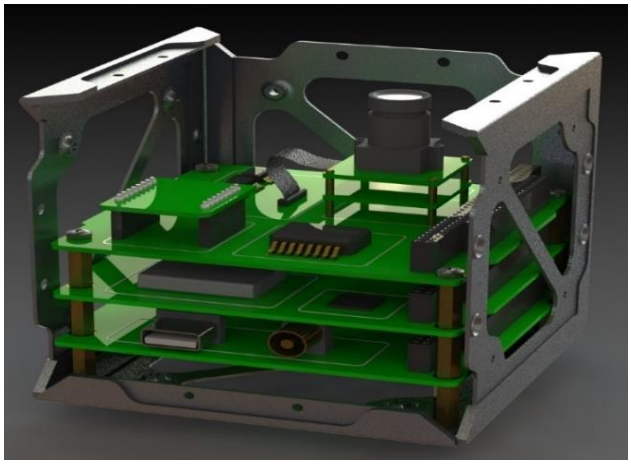

b. The inner construction of the 2 units cube satellite The inner construction of the 2 units cube satellite

Fig. 2: Two units cube satellite with its inner construction

2. Experimental Investigation MPPT Model Approach

There are many applications of the photovoltaic (PV) energy generation, such as solar-powered cars, satellites and orbiting stations in space, distant power sources for equipment, and street lighting. Unlike conventional electricity production, photovoltaic technology produces no harmful petrol emissions and is environmentally friendly.

As seen in Fig. 3, the power generated by photovoltaic is variable depending on the terminal voltage for each value of radiation and temperature. As seen in Fig. (3), there is a single Maximum Power Point tackling (MPPT) connected to every radiation and temperature. The quantity of energy generated will be significantly raised if this point is tracked to make the SA system work around it. This demonstrates the value of the MPP. To stabilize the rapid changes in weather information or load variations, tracking the MPP requires a quick and intelligent controller system. The two main parts of MPPT are the dc-dc converter and the control unit.

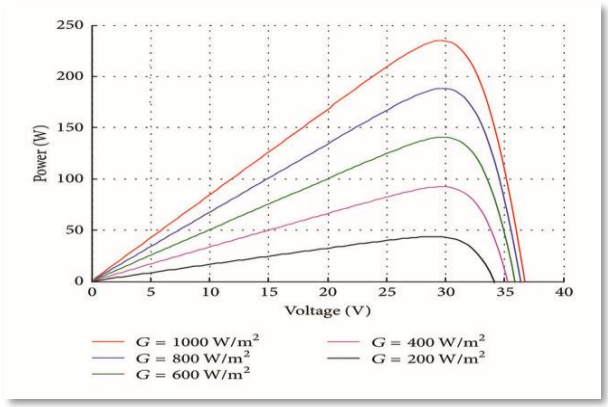

Fig. 3–PV module's P-V characteristics

PV Equivalent Circuit

In general, MPPT is used to keep track of the PV system's maximum power point. Both the MPPT circuit and the MPPT control algorithm affect MPPT efficiency. Typically, the MPPT circuit is a DC-DC converter, to which the MPPT control algorithm is applied. Fig. 4 displays a typical diagram of the MPPT connection in a PV system.

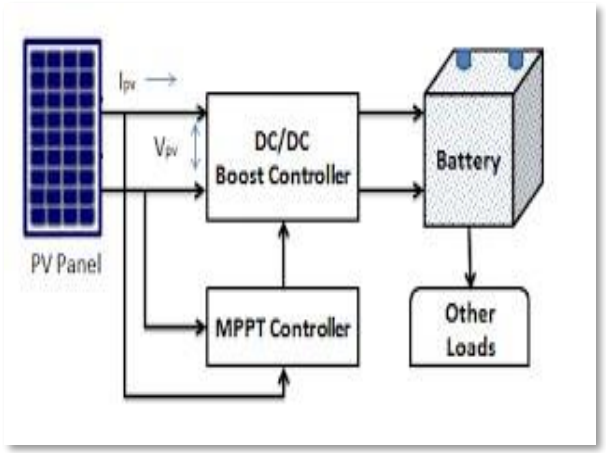

Fig. 4–PV standard schematic system with MPPT

Because the solar cell model generates DC current when exposed to light, it is categorized as a p-n semiconductor junction. It is well known among researchers that the generated current is influenced by solar irradiance, load current, and temperature. Fig. (5) depicts a typical equivalent circuit for a PV cell.

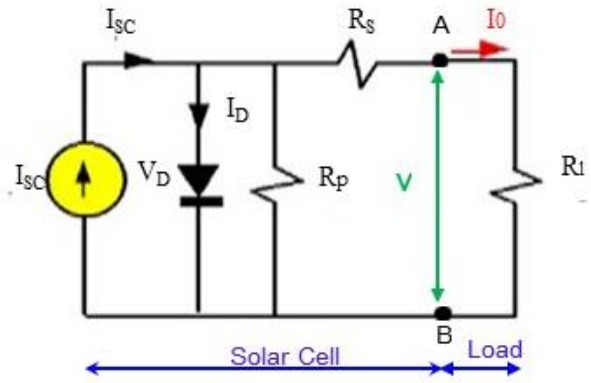

Fig. 5–Typical PV equivalent circuit

PV array Modeling

As documented in [46], the following equations clarify the PV model's I-V characteristic as:

$$I = I_{SC} - I_P - \left(\frac{V_D}{R_P}\right) - I_{PV} \quad (1)$$

$$I_D = I_0\left(e^{V_D/V_T} - 1\right) \quad (2)$$

$$V_{PV} = V_D - R_S I_{PV} \quad (3)$$

$$V_T = N_S KT/q \quad (4)$$

$$I_{PV} = \left(I_{PV_n} + K_I \Delta T\right) G/G_n \quad (5)$$

$$I_0 = \left(I_{SC,n} + K_I \Delta T\right)/\left(exp\{V_{OC,n} + K_V \Delta T/ aV_T\} - 1\right) \quad (6)$$

$$I_{PV} = [(R_S + R_P/R_P)] \times I_{SC,n} \quad (7)$$

$$\Delta T = T - Tn \quad (8)$$

where,

I_{PV} the cell's current (A);
$I_{PV,n}$ the cell's nominal current STC (25ºC and 1 kW/m^2);
I_{SC} the current generated by light (A);
I_D the current used for diode saturation (A);
R_S the series resistance of the cell (Ω);
R_P the shunt resistance of the cell (Ω);
V_D the diode's voltage (v);
V_T the temperature's voltage (v);
V_{PV} the cell's voltage (v);
ΔT the difference between the ambient temperatures measured in Kelvin (°K) and the real T and nominal STC Tn;
G the PV array's surface solar radiation intensity in Watt/m^2;
G_n the STC solar radiation intensity nominal value;
K_V, K_I the temperature coefficients of voltage and current.

The terminal electric current value is acquired by using numerical methods to solve the I-V equation iteratively, where the I-V equation is satisfied by the corresponding I value for every V value. Next, using the current system, the terminal electric current produced by the PV array is obtained for the modelling stage.

MPPT solar system

Photovoltaic energy is becoming increasingly important in the electrical power applications, as it is regarded as a limitless and widely available source of energy. Only one operating point, indicated by a localized voltage and current known as MPPT, can provide the maximum power that is available, which is an important feature of solar panels. The location is movable and varies with load, temperature, and irradiance. We must use the most solar panel watts possible due to the comparatively excessive cost of this kind of energy. To guarantee that, the maximum amount of power is produced continuously, a mechanism known as MPPT is needed for the pursuit (tracking) of the MPP. The (MPPT has been extensively tracked by the development and application of numerous traditional techniques and controllers.

The PV array converts sunlight into electrical energy. The maximum power point (MPP) of the characteristic curve of P-V denotes the point at which the module provides its maximum power output and performs at maximum efficiency (P_{max}) as shown in Fig. 6. The energy flow from the solar module to the load is interfaced by a controlled DC/DC converter to reach an operating point close to this MPP.

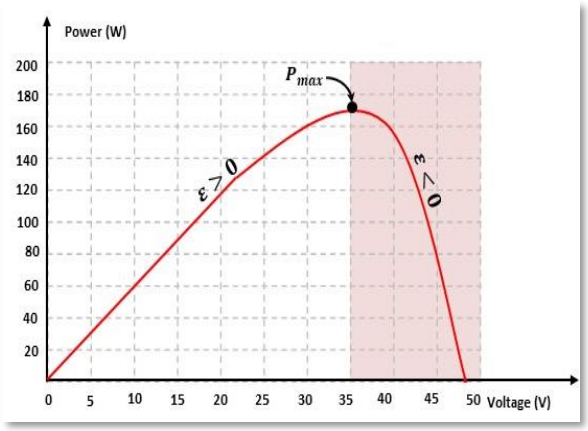

Fig. 6–Power curve with constant temperature and irradiance

3. Algorithms for MPPT

MPPT uses a specific tracking algorithm that is based on a control system. In general, the MPPT controllers are regarded as a crucial and effective component of solar power systems. They have the following benefits [47, 48]:

- Their power output increases (subject to environmental conditions).
- They are more adaptable because they can increase the voltage system by connecting solar power panels in series.
- They are economical as they do away with the requirement for gearbox wiring during PV system installation.

Effects of Irradiance (G) and Temperature (T) on PV array

From the numerical solution of the current, Equations (1) to (8) and the parameters of MATLAB program is used together with the input module in order to create the electrical I-V, P-V and R-V characteristics curves at different selected ambient temperatures T in °kelvin and sun illumination or insolation G in W/m^2 [49]. Requirements for modifying photovoltaic array models are contained in part in the datasheets provided by PV panel manufacturers; the remaining parameters are not included in those datasheets.

I-V characteristics curves for various temperatures and irradiation levels are also provided in some manufacturers' datasheets. This information is typically referred to as the nominal values of sunlight and the ambient temperature, and it is always extracted at STC. One way to assess a PV module's performance is to compare its performance with the manufacturer's specifications as stated in the STCs for the module.

Effects of Variations in Irradiance (G) on Electrical Characteristics Curves

The modelling method expresses the resulting MATLAB curves representing changes in the amount of irradiance intensity, which have a significant impact on the PV module's curves representing electrical properties, for the single chosen PV (KC200GT) module. The following levels of irradiance are considered: 835 W/m^2, 1000 W/m^2 (which is equivalent to the nominal isolation Gn), and 1350 W/m^2.

Performance of the KC200GT PV Module at 25 °C Temperature (T)

Figures (7) and (8) illustrate how the KC200GT PV module's I-V and P-V curves vary with irradiance level G while the surrounding temperature stays constant.

PV arrays' ISC rises as solar irradiation level rises and is solely and linearly dependent on irradiance level. Furthermore, the V_{oc} marginally rises as the irradiance level rises. For multicrystal KC200GT PV modules, it is approximately 26.32V for a nominal temperature of 25 °C and an irradiance of 1 kW/m^2, respectively. The array PV current increases as the irradiance level does. The electrical power generated by a PV array and the amount of irradiance are directly proportional.

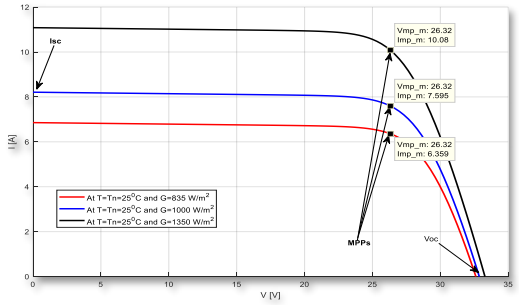

Fig. 7– I-V characteristics curve at 25 °C with varying G

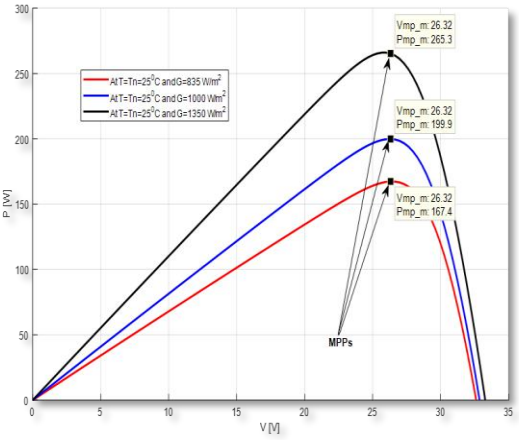

Fig. 8–P-V characteristics with varying G

When the surrounding temperature stays constant, the maximum output power rises as the irradiance level does. Changes in voltage and current determine the MPP when the irradiance level varies. The maximum power voltage rises in tandem with every increase in solar radiation. The R-V curves for both modules show that there is only a small effect of variations in the irradiance level on the output voltage.

Moreover, as irradiance increases, so does the current passing through the solar array. Its level of illumination and the PV arrays' output power are directly proportional. Moreover, at constant ambient temperature, the maximum generated power rises with the illumination level. Voltage and current variations that determine the MPP are brought on by changes to the irradiance level. The maximum power voltage usually rises in tandem with any increase in solar radiation.

KC200GT PV Module Results with 1000 W/m^2 G (AM1.5)

The simulation algorithm for the PV KC200GT module expresses the resulting MATLAB curves of ambient temperature variations, which have a considerable influence on the PV module's electrical characteristics curves. Three temperatures are considered: 25°C (the

nominal temperature Tn), 50°C, and 75°C. Figures (9) and (10) depict how the I-V and P-V curves alter with changes in ambient temperature for the KC200GT photovoltaic module when the solar irradiance level stays constant. The above-mentioned figures highlight the key variables and points of the model.

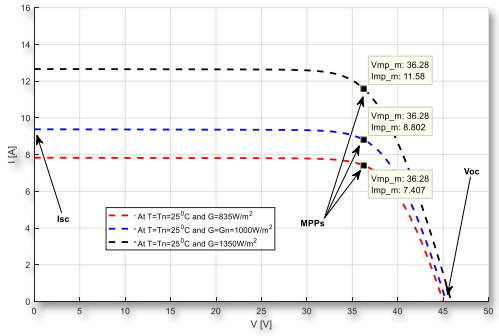

Fig. 9–The I-V Ch curve at varying T, with a G of 1000 W/m^2.

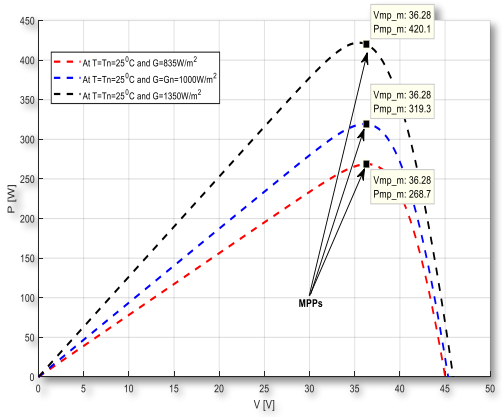

Fig. 10–The P-V Ch curve at various T and a G of 1000W/m^2.

The ISC of PV arrays is simply and linearly dependent on the irradiance level, and it rises with solar irradiation level. Furthermore, the Voc marginally rises as the irradiance level rises. For multicrystal KC200GT PV modules, it is approximately 36.28V for irradiance of 1000 W/m^2 and nominal temperature equal 25 °C. These simulation-derived results highlight that the suggested model's outcomes agree with the chosen photovoltaic module specifications that are both practical and experimental as listed in the datasheets provided by the manufacturer.

MPPT with FLC-based Charge Controller

PV panels are operated at that point (MPP) using various MPPT controller techniques, as mentioned. For the proposed approach, the FLC-based MPPT method is preferred due to its quick response to ecological conditions and independence from changes in PV array parameters. Furthermore, understanding the precise the system mathematical model is not strictly necessary for FLC to function. Fuzzy logic also has additional advantages in terms of simplicity and flexibility. Because it is based on actual system operation, it is incredibly simple to apply and implement. Furthermore, fuzzy logic can deal with issues involving imprecise and incomplete data and makes handling nonlinearities of arbitrary complexity in systems easier.

The power change rate with respect to voltage (*dP/dV*) is calculated by the FLC by analyzing the PV generates electricity at each sample time (k). Furthermore, it adjusts the PWM's duty cycle (D) so that dP/dV stays equal to zero. It illustrates the concept of the fluctuations in the rate of change throughout the PV module's curve of P-V characteristics, as seen in Fig. 11. The FLC modifies the D to increase the voltage If the value of this rate of change is greater than zero, or until the power level reaches its maximum or the dP/dV value is equal to zero. Then, the FLC modifies the D to lower the voltage up until the maximum power is achieved if this value is less than zero.

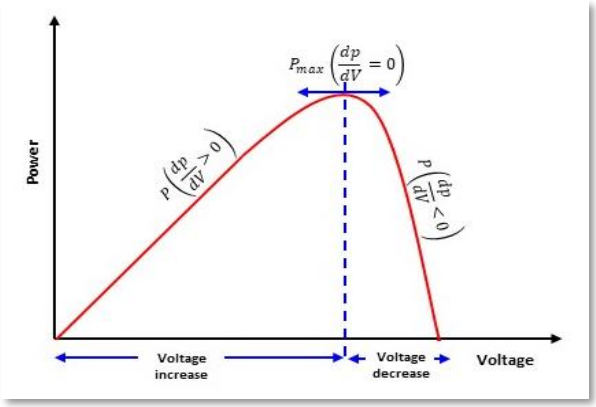

Fig. 11–The P-V characteristics curve's dP/dV variability [50].

Equations (8) and (9) model the two FLC input variables at sampled time k:

$$E(k)=\frac{[P(k)-P(k-1)]}{[V(k)-V(k-1)]}=\frac{\Delta P}{\Delta V} \quad (8)$$

$$CE(k)=E(k)-E(k-1) \quad (9)$$

where,

$P(k)$	PV array power instantaneous value;
$P(k-1)$	PV array power preceding value;
$V(k)$	PV array voltage instantaneous value;
$V(k-1)$	PV array voltage preceding value;
$E(k)$	model Eror;
$CE(k)$	Change in Error.

The input E (k) defines the load operation point at instant k, which may be on the left or right of the MPP, which also expresses the P-V characteristics curve's slope. On the other hand, the input CE (k) expresses this point's direction of

motion to modify how the load operation point and MPP match.

The Change in Duty cycle ratio (CD (k), on the other hand, is the output variable of the FLC and can have either a positive or negative value. The operating point's location on the P-V characteristics curve will determine. The commonly used COG technique, also referred to as the centre of area method , or the centroid method, is the defuzzification technique employed in this model approach. It uses membership functions to transform the inference

mechanism's fuzzy output into a crisp analogue signal. The PWM generator uses the output signal to regulate the power DC to DC converter, which in turn powers the MPP that powers the load. Equation (10) presents the duty ratio D(k)'s value computation as:

$$D(k) = D(k-1) + CD(k) \qquad (10)$$

4. The Simulator PVS model utilizing FLC-MPPT

Tracking the MPP for a fully loaded PV system requires the subsystem representing the proposed FLC-based MPPT controller to connect between the PV array and DC-to-DC converter module, as shown in Figure (12). A Simulink function block called the Advisor System Model from the National Renewable Energy Laboratory (NREL) presents the solar array and enables modelling of different PV modules/arrays [50].

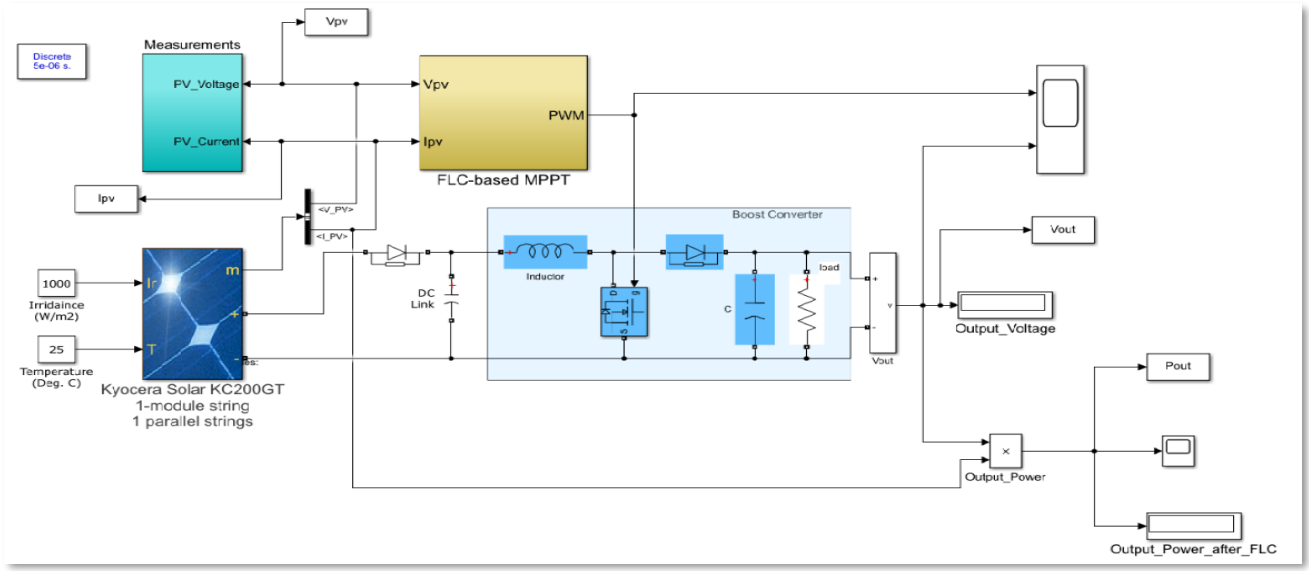

Fig. 12–Boost DC-DC Converter and FLC-MPPT in a PVS Simulink Model

Simulation Outcomes and Analysis

To assess the performance of the PV system using the FLC-Based MPPT controller, many scenarios have been created. and assessed. There are four scenarios available that replicate changes in solar radiation and abrupt shifts in the PV array's operating ambient temperature.

Scenario 1: STC with 250C temperature and 1kW/m^2 solar radiation

In the present scenario, the module was assessed under the assumptions of a 25°C ambient temperature and a nominal solar irradiance of 1000 W/m^2. Figure (13) for the KC200GT PV module displays the Vout variations against time following the application of the FLC-based MPPT algorithm. The fast response of the output voltage changes with operating time, as illustrated in Figure (13) sets apart the proposed FLC-Based MPPT controller for the PV system. because it is highly susceptible to changes in the output voltage. It can self-correct to keep the PV system stable. However, Figure (14) for the KC200GT solar power system displays Pout variations against time following the application of the FLC-based MPPT algorithm, respectively. To ensure that the PV system is stable, the output voltage changed over time, causing a rapid change in output power. This confirms the superior performance for both PV modules, as seen in Fig. (14). The fact that the chosen PV modules were used despite their power differences to illustrate this proves the validity of the suggested model. It is significant to remember that the NSS and NPP values equally were taken into consideration during the scenario simulation that we are currently working under the previously mentioned conditions. The effects of altering their values on the suggested model's performance under the same conditions are examined in the section that follows. The goal is to create a realistic PV system using a larger PV array.

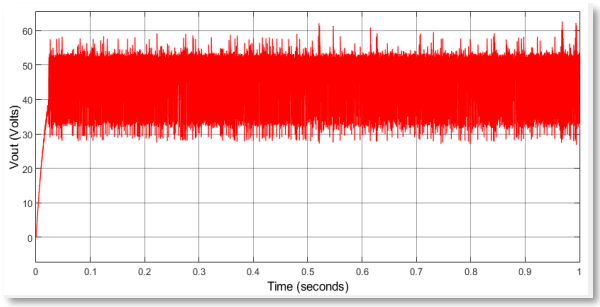

Fig. 13–Vout after FLC-Based MPPT PV System with STC

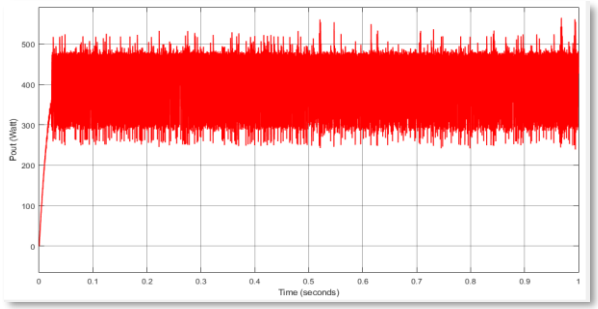

Fig. 14–Pout PV System under STC follows FLC-based MPPT.

Scenario 2: Variations in Solar Irradiance at 25°C

As shown in Figure (15), the controller's performance was assessed in this instance utilizing changes in the solar radiation on three successive states during the same time span: 835 W/m^2, 1000 W/m^2, the nominal level, and 1350 W/m^2 at a constant operating ambient temperature equal 25 °C. The variations in output power and voltage with operating time are depicted in these figures.

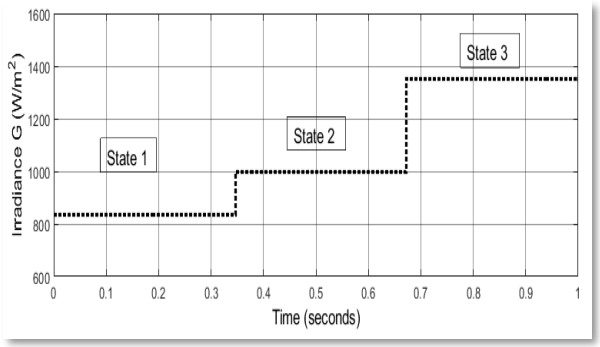

Fig. 15–Irradiance Variation Levels with constant T_n

The response of the output voltage variation (ΔVout) is high at the irradiance's low variation level (835W/m^2). Increases in irradiance levels between 835 and 1350 W/m^2 also result in increased output power variations and speed responses from the output voltage. As a result, it is discovered that the suggested PV system's speed response is sufficient to alter solar insolation to reach its stable state. The KC200GT PV array is assessed under the same conditions, and the outcomes are shown in Figures (16) and (17), respectively.

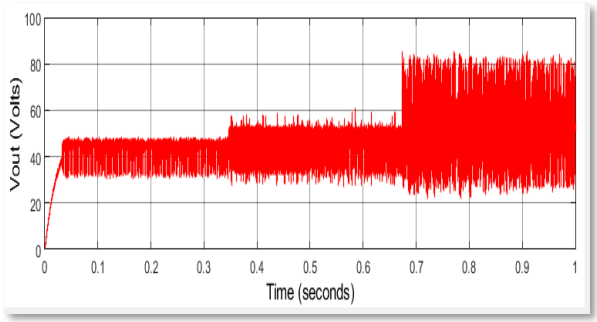

Fig. 16–Vout PV System under variable G and constant Tn following FLC-based MPPT

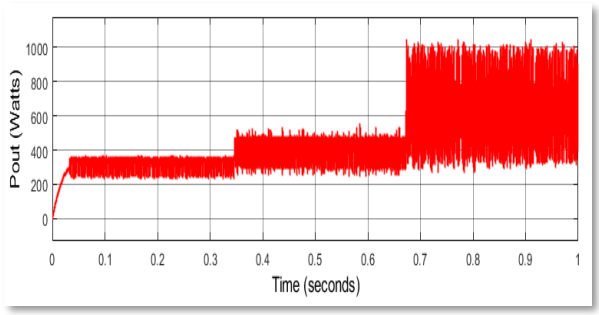

Fig. 17–Pout PV System under variable G and constant Tn following FLC-based MPPT

Similarly, when The MPPT with FLC-Based was used for the KC200GT solar system, it revealed the PV system's quick speed response under various irradiance levels. This confirmed that the suggested FLC-Based MPPT algorithm, when combined with the DC-to-DC boost converter, could keep the PV system stable and improve its performance.

Scenario 3: Variations in temperature and solar radiation at 1000 W/m^2

In the present study, the system's performance was assessed at three distinct temperatures: nominally 25°C, 50°C, and 75°C. As illustrated in Figure (18), each of these states was attained with a constant ambient solar irradiance (Gn) of 1000 W/m^2. The effects of abrupt temperature modifications to the recommended PV system's Pout and Vout for the KC200GT PV array, respectively, under continuous insolation are demonstrated in Figures (19) and (20). In Figures (19) and (20), the effect of changes in operational temperature on the proposed FLC-Based MPPT model's Pout and Vout as displayed for the KC200GT PV array under constant nominal irradiance, can be seen by examining the outcomes of the various scenarios.

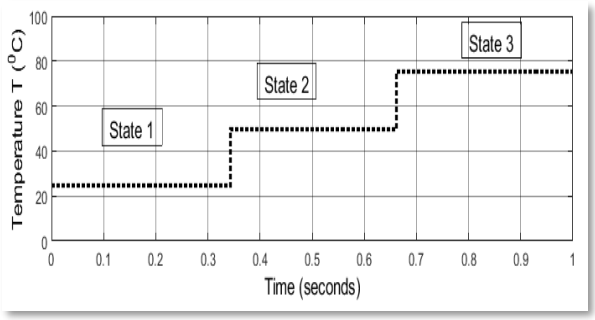

Fig. 18–Levels of Temperature Variation with Constant Gn

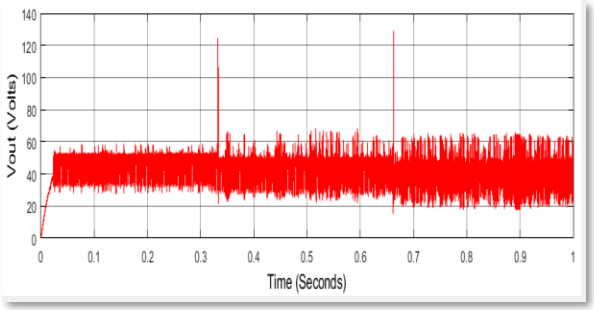

Fig. 19–Vout PV System with varying T and constant Gn following FLC-based MPPT

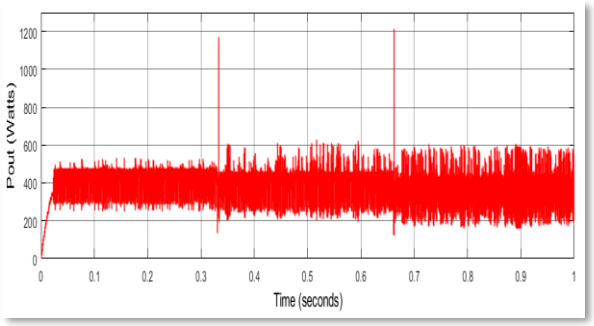

Fig. 20–Pout for PV System with variable T and constant Gn following FLC-based MPPT

Because the recommended model makes the necessary adjustments to obtain the best possible accomplishment for the PV system in real time, the impact of increasing the ambient temperature on the Pout and Vout proved that the change is insignificant and gradually implemented.

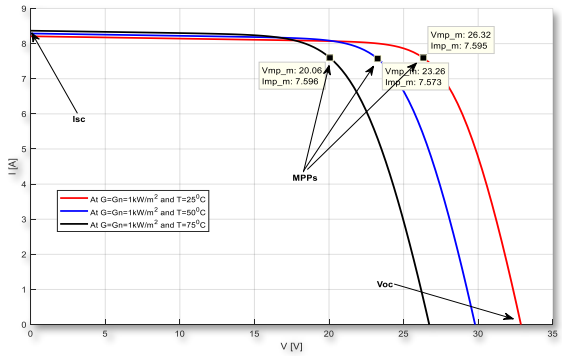

Fig. 21–I-V curves with FLCMPPT

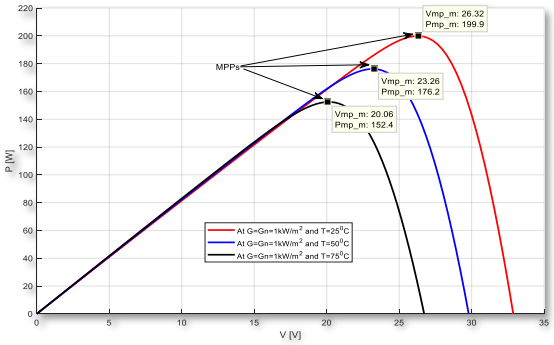

Fig. 22–P-V curve with FLCMPPT

It can be noticed from Figures (21), (22) and (23) that:

- I-V curves express that the ISC varies slightly with ambient temperature for a constant irradiance of 1kW/m^2 for multicrystal KC200GT PV modules. It is of the order of 8.2 A for irradiance of 1kW/m^2 for multicrystal KC200GT PV modules at 25 °C.
- For multicrystal KC200GT PV module, it has been noted that as temperatures rise between 25°C and 75°C, VOC levels fall in the range from approximately **32.6V to 26.5V** at 1000 W/m^2 of nominal irradiance.
- The current flowing through PV array decreases with ambient temperature. Meanwhile in the Power/Voltage curves of the module being investigated, the temperature is the main factor that reduces the PV array's peak power output at the nominal illumination level. It is observed that there is an inversely proportional relationship between temperature and maximum generated power from SA when the irradiance remains constant. It reveals that V_{MAX} decreases with ambient temperature. Therefore, the increase in T reduces the Voc.

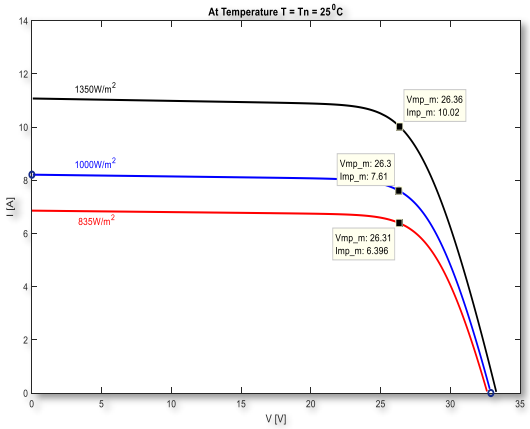

(a) I-V without FLCMPPT

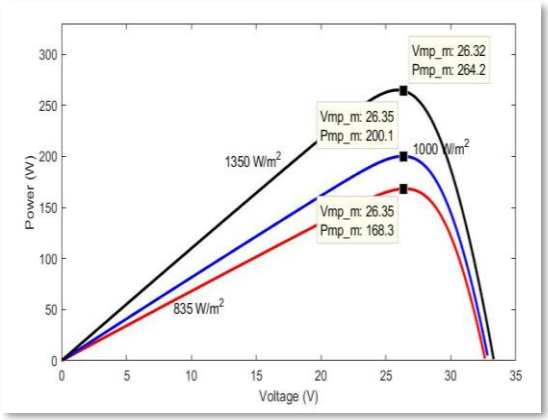

(b)) P-V without FLCMPPT

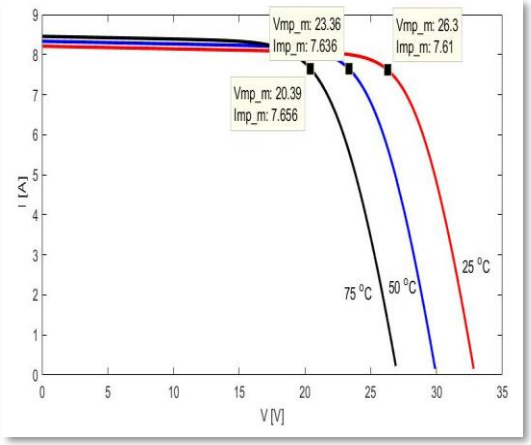

(c) I-V with FLCMPPT)

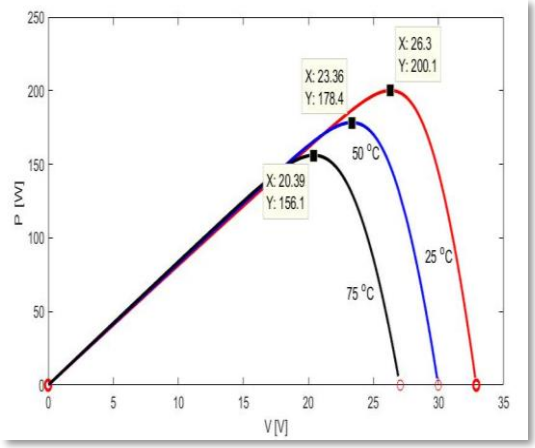

(d) P-V with FLCMPPT

Fig. 24–Performance Curves for KC200GT PV Module

Moreover, Figure (23) of the R-V characteristics for the under-study module describe the effect of temperature variations on the output voltage as obviously changes.

Figure (24) depicts the I-V and P-V characteristics for KC200GT PV Module from Simulink with and without FLCMPPT. The NSS and NPP values were equal 1 as they have been applied in the mathematical modeling stage to a PV module and not an array (NSS =1 & NPP=1) for the simplicity of the calculations. By comparing the results of the modeling and the simulation together under the same conditions, these parameters were adjusted to ensure the accuracy of the PV array model. Table 2 demonstrates a comparison between I-Vand P-V Results & Specifications of the KC200GT PV Module. As illustrated from Table 2, the simulation results, and the PV modules under study available experimental specifications, as listed in the manufacturer's datasheets, are compared, and validated with the established modelling. The above findings highlight the approximately 99.8% accuracy with a 0.02 s best response time for both the mathematical and simulation models considering the effects of varying temperatures and generation rates on the PV power of the chosen PV modules.

Table 2–I-Vand P-V Outcomes and KC200GT PV Module Specifications

I-V and P-V data for MPPs at $T=T_n=25$ °C with different G

		Mathematical modelling	Simulation	Experimental
G=835 W/m^2	V_{MP} (V)	26.32	26.32	26.3
	I_{MP} (A)	6.359	6.396	6.37
	P_{MP} (W)	167.4	168.3	167.5
G = Gn=1000 W/m^2 (STC)	V_{MP} (V)	26.32	26.32	26.3
	I_{MP} (A)	7.595	7.612	7.61
	P_{MP} (W)	199.9	200.1	200

I-V/P-V data for MPPs at $T=T_n=25$ °C & constant G

G = 1350 kW/m^2	V_{MP} (V)	26.32	26.32	26.36
	I_{MP} (A)	10.08	10.08	10.02
	P_{MP} (W)	265.3	265.3	264.2

I-V/P-V data for MPPs at different T with G of 1 kW/m^2

		Mathematical modelling	Simulation	Experimental
For T= 50 ° C	V_{MP} (V)	23.26	23.36	23.1
	I_{MP} (A)	7.573	7.636	7.62
	P_{MP} (W)	176.2	178.4	176
For T= 75 ° C	V_{MP} (V)	20.06	20.39	20.3
	I_{MP} (A)	7.596	7.656	7.63
	P_{MP} (W)	152.4	156.1	154.3

5. Experimental Results and Discussion

Experimental Set Up

The given diagram (Figure 25) shows the hardware circuit prototype. To confirm the proposed method's functionality, a prototype of the control system and the MPPT controller are created using Atmega16. They are connected either in a serial or parallel arrangement to generate a higher power value. Each configuration type offers distinct features that may be advantageous, depending on the application. The current experiment employs a PV module connected in series to attain a higher voltage.

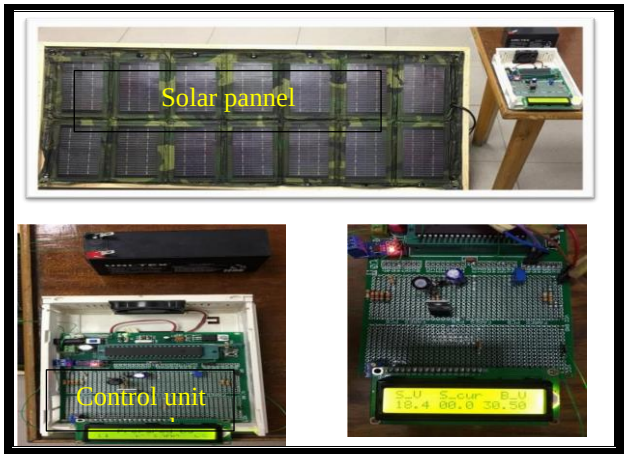

Fig. 25– Hardware circuit Prototype

The experiments were conducted with a radiation intensity of approximately 1000 watts/m^2 and a temperature

difference ranging from 25 to 60 °C. The tests were then repeated at a constant temperature of 25 °C, while the radiation intensity was varied from 835 watts/m2 to 1350 watts/m^2. The output power waveform showed variations in the form of energy waves. Figure (26) displays the variation in the output power waveform. The proposed model made appropriate adjustments to achieve optimal performance in real-time for the PV system. To assess the capability of the laboratory sample, a comparison was employed with the datasheet of MPPT controller operating in the field, the results accuracy of experimental prototype result was compared with high degree of confirmation with different environmental parameters. Table 3 shows a comparison of laboratory results and a real MPPT controller datasheet to demonstrate the quality of the experimental result. To evaluate the effectiveness of the proposed technique, it was necessary to evaluate it on a real system. The experimental tests were performed on a cubic satellite by installing a hardware prototype and connecting it to solar cells installed on the satellite. The tests were conducted in different environmental conditions, including changes in temperature (T), irradiation (G), and air mass angle (Θ).

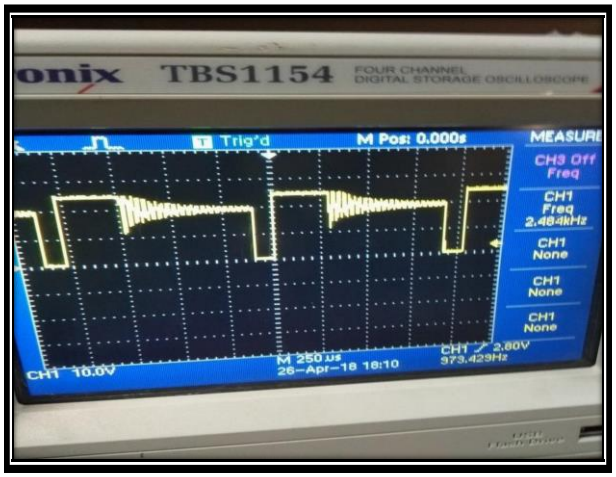

Fig. 26–Experimental results for the hardware prototype's output power wave generation.

Table 3–Performance indicators for the results of experiments.

Controller Parameters	Prototype experimental result	Datasheet value [19]
Rise time (t_r)	0.01 s	0.1 s
Settling time (t_s)	0.02 s	0.2 s
Overshoot (OV)	5.1%	5 -7%
Ripple factor (ΔP/P)	5.21 %	5.3 %

The hardware prototype demonstrated excellent results in terms of settling time and high accuracy, as shown in Table 3. The results indicate that the designed Maximum Power Point Tracking (MPPT) system can track the appropriate voltage with a response time of 0.02 seconds, while also maintaining the stability of the proposed algorithm. To ensure the validity of the proposed controller, we will compare it to existing literature in the following section.

6. A Comparison Between the Proposed Controller and The Existing Literature

In order to verify the accuracy and effectiveness of the suggested controller, we will thoroughly examine and contrast it against relevant research and studies that have been previously conducted in this field [51]. This will help us to determine the reliability and practicality of the proposed controller and provide insights into its potential limitations and areas of improvement. In this section, we consider constant temperature and variable radiation. Starting from t=1s, the irradiance shifts from 1000W/m^2 to 800W/m^2, and then drops to 600W/m^2 at t=1.5s. Figure 27 illustrates the changes in the active power output of the PV system. To simulate the solar system, we used various controller methods such as the proposed Fuzzy Logic Control (FLC), FLC improved via Particle Swarm Optimization (PSO) and Genetic Algorithm (GA), and improved FLC based on PSO and GA. We also used traditional methods such as Perturb and Observe (P&O) and INC, as described in reference [51].

In this section, we are taking constant temperature and variable radiation into account. Starting at t=1s, the irradiance changes from 1000 W/m^2 to 800 W/m^2 and then decreases to 600 W/m^2 at t=1.5s and finally it rises to 1000 W/m^2 at t=2s. Figure 27 shows the changes in the active power output of the PV system. To simulate the solar system, we used the most common controller methods such as the proposed Fuzzy Logic Control (FLC), FLC improved via Particle Swarm Optimization (PSO) and Genetic Algorithm (GA), and improved FLC based on PSO and GA. We also used traditional methods such as Perturb and Observe (P&O) and INC, as described in reference [51]. The proposed FLC offers a significant improvement in the accuracy of tracking the PV (Photovoltaic) output power.

As depicted in Figure 27 and Table 4, the active power is inversely proportional to the changes in irradiance. The FLC (Fuzzy Logic Controller) method can promptly restore the reference point and reach the Maximum Power Point (MPP) in just 0.02 seconds, while other controllers take around 0.3 seconds to reach the MPP. The PSO-GA (Particle Swarm Optimization-Genetic Algorithm) based optimized FLC generates more active power than the other controllers with lower irradiance. This controller produces 58.64 kW active power with lower irradiance, whereas other controllers produce less active power, such as 57.62 kW in the proposed FLC, 56.78 kW in PSO-based optimized FLC, 56.29 kW in INC method-based controller, 56.14 kW in GA-based optimized FLC, and 53.68 kW in P&O (Perturb and Observe) method-based controller. The

proposed FLC offers a significant improvement in the accuracy of the tracking of PV output power

Table 4–A Comparison of MPPT Controllers for various Irradiance and Constant Temperature [51].

MPPT controller	Power output (kW)			Settling time (t_s)
	1000 W/m^2	800 W/m^2	600 W/m^2	
P&O method-based controller	90.13	71.99	53.68	0.54
INC method-based controller	94.52	75.47	56.29	0.48
GA-based optimizer FLC	95.11	75.60	56.14	0.3
PSO-based optimizer FLC	96.15	76.32	56.78	0.3
PSO-GA based optimizer FLC	98.85	78.69	58.64	0.3
FLC (proposed controller)	97.25	77.40	57.62	0.02

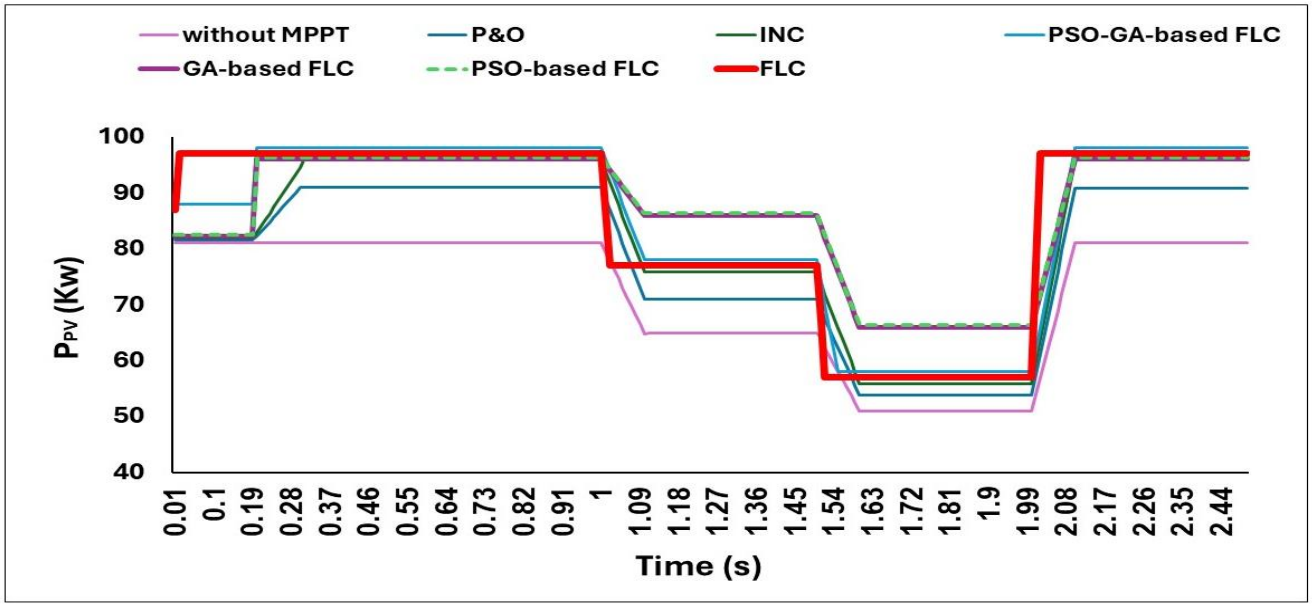

Fig. 27–A Comparison of MPPT Controllers for various Irradiance and Constant Temperature

7. CONCLUSIONS

This paper has been designed as an FLC-based MPPT controller to track the MPP and optimize the power produced by solar PV arrays. The FLC can map the peak power for each instance under varying environmental conditions, it is introduced to minimize fluctuations around the operating point, as conventional MPPT algorithms are unable to reliably monitor the MPP. To always maintain the PV output power at its maximum level, the suggested method builds an MPPT controlled by the FLC algorithm. The comparison of the results shows that the FLC-based MPPT design offered offers a fast and efficient dynamic response and is independent of any PV array parameters. It was shown that the PV system with the two chosen PV modules performs exceptionally well and robustly in the face of abrupt variations in both the operating temperature and solar irradiance levels thanks to the fuzzy controller. Furthermore, the fuzzy control outperformed high efficiency compared with the conventional controllers. These findings highlight the approximately 99.8% accuracy with a 0.02 s best response time of both the mathematical modelling and the simulation when considering the effects of varying temperatures and generation rates on the PV power of the chosen PV modules.

As an extension to the current work, we will be looking into the impact of different shading levels on the PV models. In addition to this, we need to find a solution to the common problem of oscillation in voltage and output power with FL. On the other hand, we will also be evaluating a deep learning technique as an alternative method.

8. References

[1] Ahmed Mohammed Zina, "Study and Design of Stand-Alone Photovoltaic System to Maximizing Efficiency Solar Power Using Fuzzy Logic Algorithm," International Journal of Computer Science Trends and Technology (IJCST), vol. 6, no. 5, 2018, pp. 92-94.

[2] Azmi Saleh, Ks Faiqotul Azmi, Triwahju Hardianto, and Widyono Hadi, "Comparison of MPPT fuzzy logic controller based on perturb and observe (P&O) and incremental conductance (InC) algorithm on buck-boost converter," in 2nd international conference on electrical engineering and informatics (ICon EEI), 2018: IEEE, pp. 154-158.

[3] N Hussein Selman and Jawad Radhi Mahmood, "Comparison between perturb & observe, incremental conductance and fuzzy logic MPPT techniques at different weather conditions," Int. J. Innov. Res. Sci. Eng. Technol, vol. 5, no. 7, 2016, pp. 12556-12569.

[4] Hasnaa Mohamed El-Arwash and Mohamed El-Amir Atalla, "Improving the Satellite power supply continuity using flywheel energy storage system," ERJ. Engineering Research Journal, vol. 44, no. 4, 2021, pp. 365-375.

[5] Hairul Nissah Zainudin and Saad Mekhilef, "Comparison study of maximum power point tracker techniques for PV systems," the 14th International Middle East Power Systems Conference (MEPCON'10), 2010.

[6] Badreddine Babes, Amar Boutaghane, and Noureddine Hamouda, "A novel nature-inspired maximum power point tracking (MPPT) controller based on ACO-ANN algorithm for photovoltaic (PV) system fed arc welding machines," Neural Computing and Applications, vol. 34, no. 1, 2022, pp. 299-317.

[7] Abdelghani Harrag and Hegazy Rezk, "Indirect P&O type-2 fuzzy-based adaptive step MPPT for proton exchange membrane fuel cell," Neural Computing and Applications, vol. 33, 2021, pp. 9649-9662.

[8] Hyeon-Seok Lee and Jae-Jung Yun, "Advanced MPPT algorithm for distributed photovoltaic systems," Energies, vol. 12, no. 18, 2019, p. 3576.

[9] Farhad Khosrojerdi, Shamsodin Taheri, and Ana-Maria Cretu, "An adaptive neuro-fuzzy inference system-based MPPT controller for photovoltaic arrays," in IEEE Electrical Power and Energy Conference (EPEC), 2016: IEEE, pp. 1-6.

[10] Rayane Hijazi and Nabil Karami, "Neural Network Assisted Variable-Step-Size P&O for Fast Maximum Power Point Tracking," in 32nd International Conference on Microelectronics (ICM), 2020: IEEE, pp. 1-6.

[11] Mohammad Junaid Khan and Lini Mathew, "Fuzzy logic controller-based MPPT for hybrid photo-voltaic/wind/fuel cell power system," Neural Computing and Applications, vol. 31, 2019, pp. 6331-6344.

[12] Ahmed G Abdullah, Mothanna Sh Aziz, and Bashar A Hamad, "Comparison between neural network and P&O method in optimizing MPPT control for photovoltaic cell," International Journal of Electrical & Computer Engineering (2088-8708), vol. 10, no. 5, 2020.

[13] Mohammad Sarvi and Ahmad Azadian, "A comprehensive review and classified comparison of MPPT algorithms in PV systems," Energy Systems, vol. 13, no. 2, 2022, pp. 281-320.

[14] Parag K Atri, Ps Modi, and Nikhil Shashikant Gujar, "Comparison of different MPPT control strategies for solar charge controller," in International Conference on Power Electronics & IoT Applications in Renewable Energy and its Control (PARC), 2020: IEEE, pp. 65-69.

[15] Ihssane Chtouki, Patrice Wira, and Malika Zazi, "Comparison of several neural network perturb and observe MPPT methods for photovoltaic applications," in IEEE International Conference on Industrial Technology (ICIT), 2018: IEEE, pp. 909-914.

[16] Mahyar Khosravi, Saeed Heshmatian, Davood A Khaburi, Cristian Garcia, and Jose Rodriguez, "A novel hybrid model-based MPPT algorithm based on artificial neural networks for photovoltaic applications," in IEEE Southern Power Electronics Conference (SPEC), 2017: IEEE, pp. 1-6.

[17] Anil Kumar Dahiya, "Implementation and Comparison of Perturb & Observe, ANN and ANFIS Based MPPT Techniques," in international conference on inventive research in computing applications (ICIRCA), 2018: IEEE, pp. 1-5.

[18] Zuhair Alaas, Galal Eldin A Eltayeb, Mujahed Al-Dhaifallah, and Mohsen Latifi, "A new MPPT design using PV-BES system using modified sparrow search algorithm based ANFIS under partially shaded conditions," Neural Computing and Applications, vol. 35, no. 19, 2023, pp. 14109-14128.

[19] Khaled Bataineh, "Improved hybrid algorithms-based MPPT algorithm for PV system operating under severe weather conditions," IET Power Electronics, vol. 12, no. 4, 2019, pp. 703-711.

[20] Sajid Sarwar, Muhammad Yaqoob Javed, Mujtaba Hussain Jaffery, Jehangir Arshad, Ateeq Ur Rehman, Muhammad Shafiq, and Jin-Ghoo Choi, "A novel hybrid MPPT technique to maximize power harvesting from pv system under partial and complex partial shading," Applied Sciences, vol. 12, no. 2, 2022, p. 587.

[21] Hassna M. El Arwash Mohamed El Amir Attalla, "Improving Solar Cell System Performance using Fuzzy Logic MPPT Technique under Environmental Condition Variations," INTERNATIONAL JOURNAL OF ENGINEERING RESEARCH & TECHNOLOGY (IJERT), vol. 10, no. 6 2021, doi: 10.17577/IJERTV10IS060278.

[22] Ratnakar Babu Bollipo, Suresh Mikkili, and Praveen Kumar Bonthagorla, "Hybrid, optimal, intelligent and classical PV MPPT techniques: A review," CSEE Journal of Power and Energy Systems, vol. 7, no. 1, 2020, pp. 9-33.

[23] Said Azzouz, Sabir Messalti, and Abdelghani Harrag, "A Novel Hybrid MPPT Controller Using (P&O)-neural Networks for Variable Speed Wind Turbine Based on DFIG. Model," Meas. Control A, vol. 92, 2019, pp. 23-29.

[24] M Arjun and Jb Zubin, "Artificial neural network based hybrid MPPT for photovoltaic modules," in International CET Conference on Control, Communication, and Computing (IC4), 2018: IEEE, pp. 140-145.

[25] Slimane Hadji, Jean-Paul Gaubert, and Fateh Krim, "Real-time genetic algorithms-based MPPT: study and comparison (theoretical an experimental) with conventional methods," Energies, vol. 11, no. 2, 2018, p. 459.

[26] Arfaoui Jouda, Feki Elyes, Abdelhamid Rabhi, and Mami Abdelkader, "Optimization of scaling factors of fuzzy–MPPT controller for stand-alone photovoltaic system by particle swarm optimization," Energy Procedia, vol. 111, 2017, pp. 954-963.

[27] Hong Li, Duo Yang, Wenzhe Su, Jinhu Lü, and Xinghuo Yu, "An overall distribution particle swarm optimization MPPT algorithm for photovoltaic system under partial shading," IEEE Transactions on Industrial Electronics, vol. 66, no. 1, 2018, pp. 265-275.

[28] Doudou N Luta and Atanda K Raji, "Fuzzy rule-based and particle swarm optimisation MPPT techniques for a fuel cell stack," Energies, vol. 12, no. 5, 2019, p. 936.

[29] Laxman Bhukya, Narender Reddy Kedika, and Surender Reddy Salkuti, "Enhanced maximum power point techniques for solar photovoltaic system under uniform insolation and partial shading conditions: a review," Algorithms, vol. 15, no. 10, 2022, p. 365.

[30] Ke Guo, Lichuang Cui, Mingxuan Mao, Lin Zhou, and Qianjin Zhang, "An improved gray wolf optimizer MPPT algorithm for PV system with BFBIC converter under partial shading," Ieee Access, vol. 8, 2020, pp. 103476-103490.

[31] Suresh Srinivasan, Ramji Tiwari, Murugaperumal Krishnamoorthy, M Padma Lalitha, and K Kalyan Raj, "Neural network based MPPT control with reconfigured quadratic boost converter for fuel cell application," International Journal of Hydrogen Energy, vol. 46, no. 9, 2021, pp. 6709-6719.

[32] Muhammad Rameez Javed, Aashir Waleed, Umar Siddique Virk, and Syed Zain Ul Hassan, "Comparison of the adaptive neural-fuzzy interface system (ANFIS) based solar maximum power point tracking (MPPT) with other solar MPPT methods," in IEEE 23rd international multitopic conference (INMIC), 2020: IEEE, pp. 1-5.

[33] Moirangthem Dennis Singh, Vj Shine, and Varaprasad Janamala, "Application of artificial neural networks in optimizing MPPT control for standalone solar PV system," in international conference on contemporary computing and informatics (IC3I), 2014: IEEE, pp. 162-166.

[34] Jobeda Khanam and Simon Y Foo, "Neural networks technique for maximum power point tracking of photovoltaic array," in SoutheastCon 2018: IEEE, pp. 1-4.

[35] Wafa Hayder, Dezso Sera, Emanuele Ogliari, and Abderezak Lashab, "On Improved PSO and Neural Network P&O Methods for PV System under Shading and Various Atmospheric Conditions," Energies, vol. 15, no. 20, 2022, p. 7668.

[36] Idriss Dagal, Burak Akın, and Erdem Akboy, "MPPT mechanism based on novel hybrid particle swarm optimization and salp swarm optimization algorithm for battery charging through simulink," Scientific reports, vol. 12, no. 1, 2022, p. 2664.

[37] Ziad M Ali, Thamer Alquthami, Salem Alkhalaf, Hojat Norouzi, Sajjad Dadfar, and Kengo Suzuki, "Novel hybrid improved bat algorithm and fuzzy system based MPPT for photovoltaic under variable atmospheric conditions," Sustainable Energy Technologies and Assessments, vol. 52, 2022, p. 102156.

[38] Linjuan Gong, Guolian Hou, and Congzhi Huang, "A two-stage MPPT controller for PV system based on the improved artificial bee colony and simultaneous heat transfer search algorithm," ISA transactions, vol. 132, 2023, pp. 428-443.

[39] Saibal Manna, Ashok Kumar Akella, and Deepak Kumar Singh, "A novel MRAC-MPPT scheme to enhance speed and accuracy in PV systems," Iranian Journal of Science and Technology, Transactions of Electrical Engineering, vol. 47, no. 1, 2023, pp. 233-254.

[40] Saibal Manna, Deepak Kumar Singh, Ashok Kumar Akella, Ay Abdelaziz, and Miska Prasad, "A novel robust model reference adaptive MPPT controller for Photovoltaic systems," Scientia Iranica, 2022, doi: 10.24200/SCI.2022.59553.6312.

[41] Hadeed Ahmed Sher, Ali Faisal Murtaza, Abdullah Noman, Khaled E Addoweesh, Kamal Al-Haddad, and Marcello Chiaberge, "A new sensorless hybrid MPPT algorithm based on fractional short-circuit current measurement and P&O MPPT," IEEE Transactions on sustainable energy, vol. 6, no. 4, 2015, pp. 1426-1434.

[42] M Berrera, A Dolara, R Faranda, and Sonia Leva, "Experimental test of seven widely-adopted MPPT algorithms," in IEEE Bucharest PowerTech, 2009: IEEE, pp. 1-8.

[43] Bidyadhar Subudhi and Raseswari Pradhan, "A comparative study on maximum power point tracking techniques for photovoltaic power systems," IEEE transactions on Sustainable Energy, vol. 4, no. 1, 2012, pp. 89-98.

[44] T Meschede and J Rießelmann, "Development of ACS, Payloads and Subsystems for modular Satellites Using a Hybrid Test Bed," https://robotics.estec.esa.int/i-

SAIRAS/isairas2016/Session8a/S-8a-3-ThomasMeschede.pdf.

[45] Mohamed Alam, Anas Khamees, Tarek Aboelnaga, Abdelrahman Amer, Ahmed Harbi, Mohamed Alamir, Hassnaa Alarwsh, and Osama A Elsayed, "Design and Implementation of an Onboard Computer and payload for Nano Satellite (CubeSat)," in The International Undergraduate Research Conference, 2021, vol. 5, no. 5: The Military Technical College, pp. 361-364, doi: https://doi.org/10.21608/IUGRC.2021.246386.

[46] Ali Reza Reisi, Mohammad Hassan Moradi, and Shahriar Jamasb, "Classification and comparison of maximum power point tracking techniques for photovoltaic system: A review," Renewable and sustainable energy reviews, vol. 19, 2013, pp. 433-443.

[47] Carlos Robles Algarín, John Taborda Giraldo, and Omar Rodriguez Alvarez, "Fuzzy logic based MPPT controller for a PV system," Energies, vol. 10, no. 12, 2017, p. 2036.

[48] Haider Ibrahim and Nader Anani, "Variations of PV module parameters with irradiance and temperature," Energy Procedia, vol. 134, 2017, pp. 276-285.

[49] Basil M Hamed and Mohammed S El-Moghany, "Fuzzy controller design using FPGA for photovoltaic maximum power point tracking," International Journal of Advanced Research in Artificial Intelligence, vol. 1, no. 3, 2012, pp. 14-21.

[50] Nate Blair, Aron P Dobos, Janine Freeman, Ty Neises, Michael Wagner, Tom Ferguson, Paul Gilman, and Steven Janzou, "System advisor model, sam 2014.1. 14: General description," National Renewable Energy Lab.(NREL), Golden, CO (United States).

[51] Majid Dehghani, Mohammad Taghipour, Gevork B Gharehpetian, and Mehrdad Abedi, "Optimized fuzzy controller for MPPT of grid-connected PV systems in rapidly changing atmospheric conditions," Journal of Modern Power Systems and Clean Energy, vol. 9, no. 2, 2020, pp. 376-383.